Hydrodynamic conditioning of aluminium–bentonite flocs

C. Coufort and A. Liné

Laboratoire d'Ingénierie des Procédés de l'Environnement, INSA Toulouse, 135 Avenue de Rangueil 31077 Toulouse Cedex 4 France (E-mail: *carole.coufort@insa-toulouse.fr; alain.line@insa-toulouse.fr*)

Abstract The aim of this paper is to analyse the role of hydrodynamics in flocculation. The effects of a hydrodynamic sequencing (flocculation–break-up–reflocculation–break-up–reflocculation) on the evolution of aluminium–bentonite floc size distributions and structure are investigated by image analysis in a Taylor–Couette reactor. The flocculation phenomena analysed in this study mainly occur in the viscous subrange, with floc size below the Kolmogorov micro-scale. The high sensitivity of steady-state floc size distribution to initial floc size distribution (elementary particles or flocs formed issuing break-up stages) is highlighted. Reversibility or irreversibility of agglomeration and break-up phenomena are discussed in terms of floc history and hydrodynamic stress. Finally, the hydrodynamic conditioning for aluminium–bentonite flocs is examined.

Keywords Cycled flocculation; floc size distribution; hydrodynamics; Kolmogorov length-scale

Introduction

The removal of tiny particles is essential to water treatment and is generally achieved through a flocculation process. The flocculation of colloidal particles can be divided into two steps: (1) a coagulant (aluminium sulphate for example) is injected to destabilise particles and decrease the energy barrier. The main requirement is for the additive to be distributed uniformly and rapidly among the suspension and this is achieved by a high mixing rate; (2) flocculation of destabilised particles that is mainly related to collisions induced by lower mixing and limited by the break-up of larger flocs.

Agglomeration

Particle collisions occur primarily thanks to the shear of the fluid and are directly related to local velocity gradients. Expressions for the local velocity gradients can be found in the work of Thomas (1964). They depend on the size of the flocs in comparison with the size of the Kolmogorov length-scale (η).

$$\eta = (\nu^3/\varepsilon)^{1/4}$$

where ν is the kinematic viscosity and ε the viscous dissipation rate of turbulent kinetic energy. The Kolmogorov length-scale is the smallest size of eddies at which the turbulent kinetic energy is dissipated by viscosity. Initial colloid particles are extremely small in relation to η. Therefore, flocculation mainly occurs in the viscous subrange, which means below the Kolmogorov length-scale. For this reason, the modeling of agglomeration involves hydrodynamic parameters. Derived from Smoluchowski theory, the most common model of the collision frequency assumes that particles move in straight lines until collisions occur. The collision frequency of two particles of radii r_i and r_j has the following formulation:

$$\beta(i,j) = 4/3\sqrt{\varepsilon/\nu}(r_i + r_j)^3$$

doi: 10.2166/ws.2006.002

Water Science and Technology: Water Supply **Vol 6 No 1 pp 11–19** © INSA Toulouse 2006

In the present work, the physico-chemical conditions are fixed; so the collision efficiency is considered as constant.

Break-up

As flocs grow, the hydrodynamic stress can lead to break-up of the floc into several fragments or to erosion. The break-up phenomena can be analyzed with the following ratio:

$$B = \frac{\text{hydrodynamic force}}{\text{cohesion force}} = \frac{F}{J}$$

where F is the force exerted on the floc by the hydrodynamics and J represents the aggregate strength. If B is lower than 1, the particle withstands the hydrodynamic force. On the contrary ($B > 1$), the hydrodynamic force breaks up the floc. The cohesion force is related to physico-chemical conditions and aggregate structure while the hydrodynamic force is generally estimated as:

$$F \approx \sigma d^2$$

where d^2 stands for the area of the particle and σ the hydrodynamic stress exerted on the aggregate.

Once more, the expression of σ depends on the size of the aggregate in comparison with the size of the Kolmogorov length-scale (η). However, whatever the size of the aggregate, Bouyer *et al.* (2004) showed that for a fixed aggregate strength, floc size only depends on the viscous dissipation rate of the turbulent kinetic energy (ε):

$$d \approx \varepsilon^{-1/4}$$

Thus, for fixed physicochemical conditions, agglomeration and break-up phenomena are directly linked to hydrodynamics. To confirm the relation between floc size distribution and hydrodynamics, a sequencing made of successive low and high hydrodynamic stress periods can be applied. Several studies (Clark and Flora, 1991; Jung *et al.*, 1996; Spicer *et al.*, 1998) have already focused their attention on the effect of cycled flocculation (flocculation–break-up–reflocculation). They found that a floc grown under mixing conditions, broken up and regrown under the same mixing conditions does not have the same size and structure as the original floc prior to break-up.

Objectives

This study focuses on the influence of successive break-up and reflocculation sequences on floc size distribution, for fixed physicochemical conditions. The first flocculation step (particle destabilisation) is outside the scope of this study and is considered as non-limiting. First the influence of hydrodynamics on floc size distribution and structure is studied. Then, differences between flocculation and reflocculation stages are shown and explained, in terms of floc history and hydrodynamic stress. The final goal is to determine the influence of a break-up stage on flocculation and to establish whether an hydrodynamic conditioning of flocs can be achieved with such a cycled flocculation.

Materials and methods

Taylor–Couette reactor. The Taylor–Couette reactor consists of a pair of concentric cylinders. The inner one is rotating whereas the outer one is fixed. The radius of the inner cylinder is 100 mm (r_i) and the radius of the outer cylinder is 115 mm (r_e), resulting in a gap of 15 mm. The height of the reactor is 200 mm. For such an apparatus, the dimensionless characteristic number is the Taylor number (Ta), which compares the

inertial forces to the viscosity forces, written as:

$$Ta = \frac{\Omega_i^2 r_i (r_e - r_i)^3}{\nu^2}$$

The laminar regime (Couette flow) is characterised by a purely tangential flow in the annular gap. The first transition of flow regime occurs at $Ta \approx 1{,}700$; a series of regularly spaced toroidal vortices appear along the cylinder axis. The flow becomes more and more turbulent as Ta increases (Kataoka, 1986). The vortices remain present till $Ta \approx 1.6 \times 10^9$. Beyond this value, they disappear (Coles, 1965).

During the experiments, the rotation speed of the inner cylinder varied from 17 to 110 rpm, corresponding to Taylor numbers between 10^6 and 4.5×10^7. Thus, the flow is turbulent.

Hydrodynamic study of this apparatus can be found in Coufort (2004). Distributions of ε and η have been calculated. Two peaks are detected in the distribution of η. The smaller one corresponds to low values of η near the wall where dissipation rate of the turbulent kinetic energy (ε) is maximum. The second peak corresponds to the most probable value of the Kolmogorov length-scale in the reactor, especially in the bulk between the two cylinders. The most probable values, corresponding to the peak of the distribution (ε_{peak} and η_{peak}) are summarised in Table 1.

Suspension. A synthetic suspension of bentonite is used, at a concentration of 30 mg/l. The particles are directly injected into the Taylor–Couette reactor filled with demineralised water. Flocculation is enhanced by aluminium sulphate ($Al_2(SO_4)_3.18H_2O$) (Aldrich Chemical Company, Inc.). The concentration of aluminium sulphate is optimised to 4.0×10^{-4} mol/L Al^{3+}. Because demineralised water is used, the injection of aluminium sulphate acidifies the solution, its pH approaching 3.5. Such physicochemical conditions enable the rapid creation of flocs that can be easily analysed by image processing.

Image analysis. Floc size is determined by image analysis. This technique is based on three steps: (i) illuminating a plane of the tank with a light sheet in order to visualise flocs; (ii) recording the image of the flocs using a digital CCD camera; (iii) processing the images by an image analysis software. Images give two-dimensional information. An equivalent floc diameter is derived using the following relation:

$$d = (4A/\pi)^{1/2}$$

where A stands for the projected area of the floc on the image. The system has been validated using calibrated glass spheres whose size corresponds to the bentonite floc size, between 100 and 400 μm (Bouyer *et al.*, 2004). The population is analysed in terms of distribution (in number or weighted by size). The distribution in number directly represents the floc population. Nevertheless, as the size of the smallest particles detected by the system is about 15 μm, the small sizes must be carefully analysed. The distribution weighted by size focuses on the largest flocs and constitutes the main point of the study.

Table 1 Hydrodynamic parameters for the Taylor–Couette reactor

Ω (rpm)	17	22	36	65
η_{peak} (μm)	460	360	290	180
ε_{peak} (m^2/s^3)	3.5×10^{-5}	8.4×10^{-5}	1.4×10^{-4}	9.5×10^{-4}

Hydrodynamic sequencing. This work focuses on the influence of successive break-up and reflocculation sequences on floc size distribution for fixed physico-chemical conditions. Hydrodynamic conditions for the cycled flocculation are indicated in Figure 1. After 3 minutes of initial destabilisation of a synthetic suspension of bentonite with aluminium sulphate (stage 1), the following steps are carried out: flocculation at slow mixing speed for 45 minutes (stage 2) ($\Omega_{slow} = 17$ rpm or 22 rpm or 36 rpm); break-up at high mixing speed ($\Omega_{high} = 65$ rpm) for 30 minutes (stage 3); reflocculation for 45 minutes at Ω_{slow} (step 4), break-up at $\Omega_{high} = 65$ rpm for 30 minutes (stage 5); reflocculation for 45 minutes at Ω_{slow} (step 6).

Results

Flocculation and reflocculation stages

Floc size distributions (in number and weighted by area) at the end of stages 2 and 4 (flocculation and first reflocculation stages) are presented in Figure 2. It is found that the larger the rotation speed during the flocculation, the smaller the floc size. In addition, results show that for identical hydrodynamic conditions, floc size is always larger during stage 2 than during stage 4.

Figure 3 illustrates floc size distributions at the end of flocculation and reflocculation stages (i.e. 2, 4 and 6) in the case of $\Omega_{slow} = 22$ rpm. It can be noticed that at the end of reflocculation stages (4 and 6), for identical hydrodynamic conditions, floc size distributions are very similar and thus reproducible.

Break-up stages

Whatever the low mixing speed (17, 22 or 36 rpm), the high mixing speed during stages 3 and 5 is constant at 65 rpm. Figure 4 presents floc size distributions at the end of stage 3. Flocs are smaller than at the end of flocculation or reflocculation stages, a period of intense mixing breaks up flocs. The results also show that the system reaches the same steady-state for the different flocculation experiments, whatever the rotation speed of the inner cylinder during stages 2 and 4.

Concerning the break-up stages (stages 3 and 5), distributions for a rotation speed of the inner cylinder of 22 rpm are shown in Figure 5. Stages 3 and 5 are performed at the same high rotation speed (65 rpm). Once more, it can be noticed that floc size distributions are very close to each other, thus once a high mixing is applied, results are reproducible.

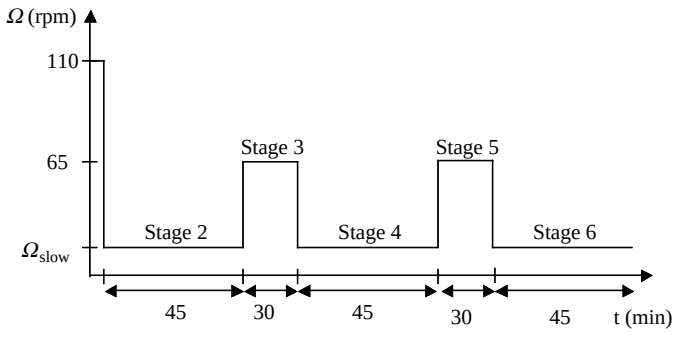

Figure 1 Schematic of hydrodynamic sequencing

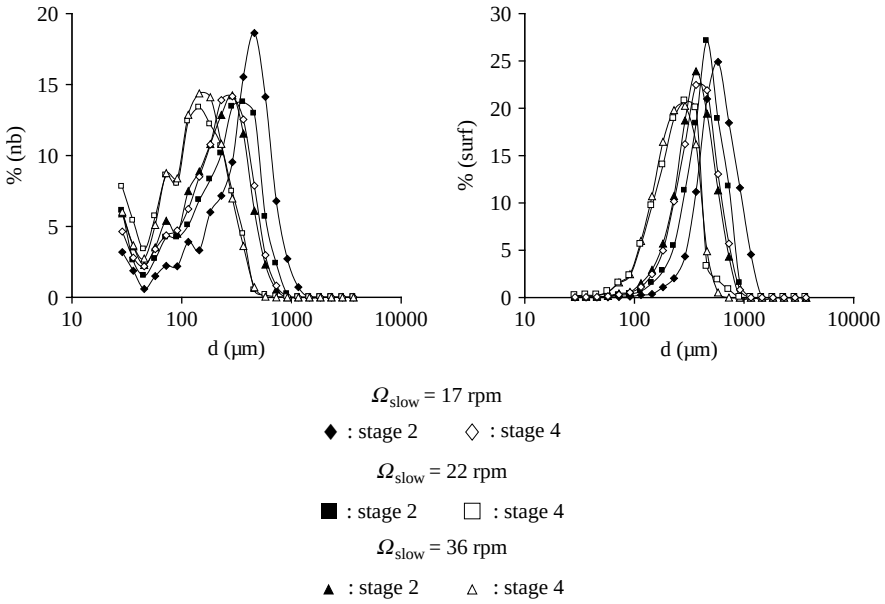

Figure 2 Floc size distributions at the end of stages 2 and 4

Relation between hydrodynamics and floc size

Results can be post-processed in terms of the relation between hydrodynamics and most probable floc size (d_{peak}) which corresponds to the peak of floc size distribution (in area). Figure 6 shows the most probable floc size versus ε_{peak} and η_{peak}.

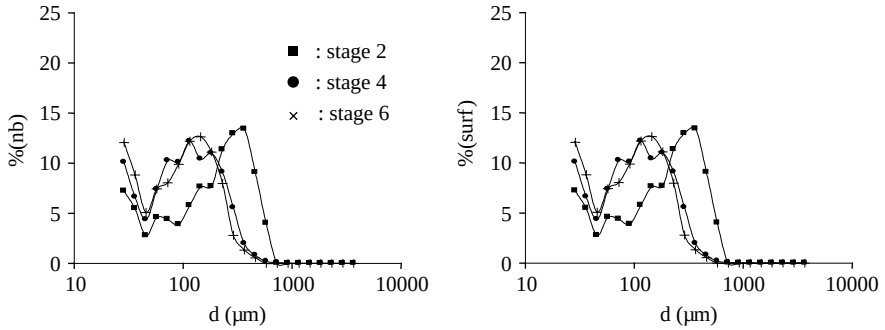

Figure 3 Floc size distributions at the end of stages 2, 4 and 6 ($\Omega_{slow} = 22$ rpm)

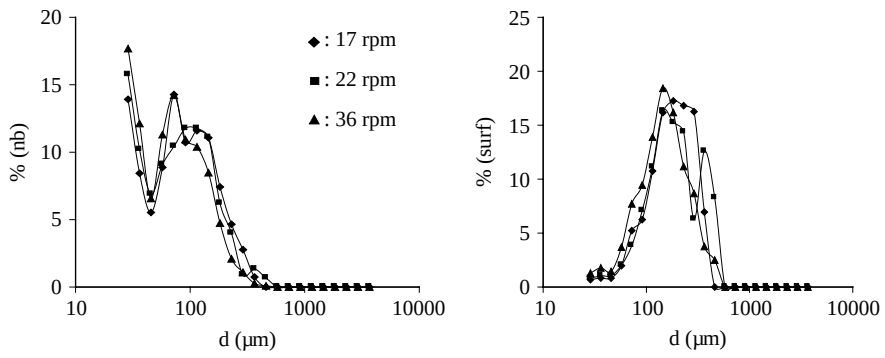

Figure 4 Floc size distributions at the end of stage 3

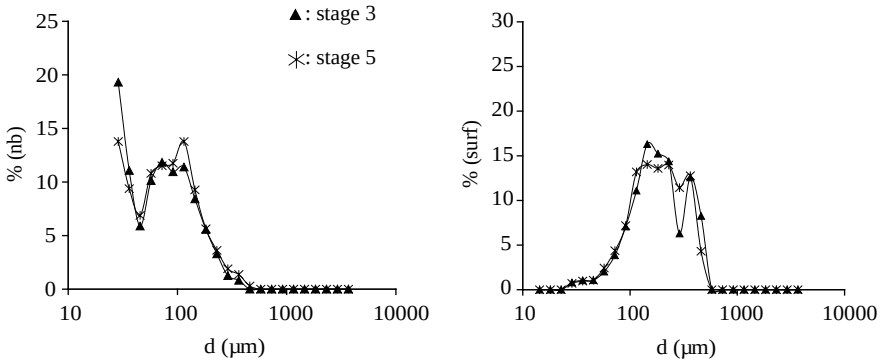

Figure 5 Floc size distributions at the end of stages 3 and 5 ($\Omega_{slow} = 22$ rpm)

Figure 6(a) shows the relationship between d_{peak} and ε_{peak} as $d_{peak} \propto \varepsilon_{+\,peak}^{-1/4}$. This result is consistent with the trend found by many investigators (Thomas, 1964; Parker *et al.*, 1972; Tambo and Watanabe, 1979; Bouyer *et al.*, 2004) and is in accordance with the expected behaviour based on the ratio B. Two distinct datasets are noticeable; the first one corresponds to stages 1 and 2 (i.e. before high mixing, stage 3); the second one to break-up and reflocculation stages. Figure 6(b) illustrates how the d_{peak} varies with η_{peak}. Whatever the slow mixing rotation speed, the most probable floc size is larger than the most probable Kolmogorov micro-scale during the flocculation stage. Concerning the reflocculation and break-up stages, floc size is close to η_{peak}.

Discussion

Sensitivity of flocculation and reflocculation stages to initial population conditions

Experimental results underline that the steady-state floc sizes differ for identical hydrodynamic conditions (stages 2 and 4). At the beginning of stage 2, the population consists of destabilised primary particles and little flocs stem from the rapid mixing. At the beginning of stage 4, the population is made up of flocs derived from the break-up phenomena of stage 3.

As a consequence, if the initial population distributions are different, the resulting floc size distributions also differ. However, if the initial populations are similar

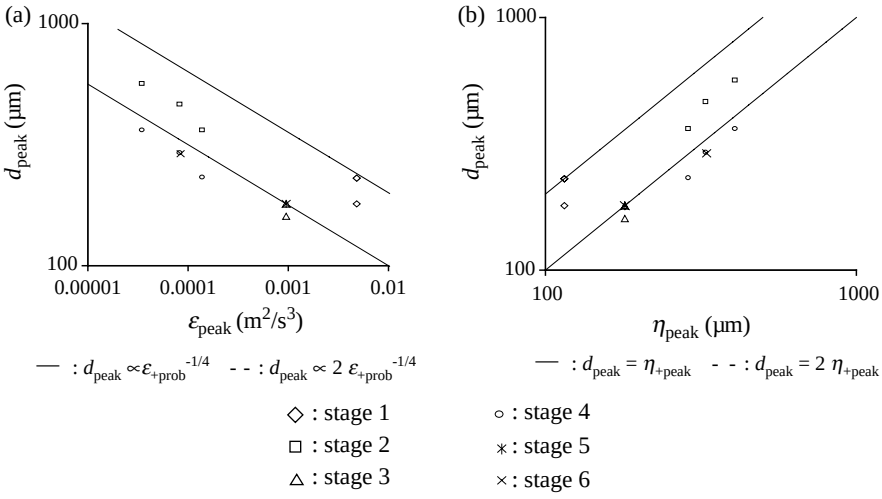

Figure 6 Most probable floc size versus $\varepsilon_{+\,peak}$ (a) and $\eta_{+\,peak}$ (b)

(stages 3 and 5), so are the steady-state populations. This result suggests that the flocculation process is very sensitive to initial population conditions.

Influence of break-up stages on floc size and structure

At the end of stage 3 (Figure 4), the floc size distributions have similar shapes whatever the mixing speed of the previous stage. Rupture phenomena are thus independent of the initial floc size. In addition, the most probable floc size is close to η_{peak} which represents the size of the smallest eddies dissipating the energy. So, large floc size is mainly determined by hydrodynamics. More precisely floc size is closely linked with turbulence and especially with the dissipation of turbulent kinetic energy (ε).

Concerning the influence of break-up stages on floc structure, the total area occupied by flocs on the images in the course of the hydrodynamic sequencing can be analysed. The results are reported in Figure 7. The physico-chemical conditions are exactly the same for the three experiments.

As the total mass of bentonite does not vary during the experiments, a reduction in the area occupied by the flocs on the images indicates a compaction of the structure. As expected, for flocculation stages, the lower the rotation speed of the inner cylinder, the looser are the aggregates formed.

During the break-up step (stage 3), the total surface decreases. This result indicates that the floc structure changes, aggregates become denser. Concerning the reflocculation stages, the same remark can be added. Spicer *et al.* (1998) studied the effect of flocculation–break-up–reflocculation steps on the evolution of flocculation. They found that a hydrodynamic stress, exerted by a break-up stage, compacts the floc structure. This modification is experimentally evaluated by the increase of the mass fractal dimension during a break-up stage. The present results are in accordance with this work. Hence, a break-up stage calibrates not only the size but also the floc structure.

Mechanisms

Experimental results show that flocs reach a larger size during the flocculation stage than during reflocculation stages. The rupture stage influences floc size and structure independently of floc size prior to the break-up. A new kind of aggregate is created: the flocculi. After the break-up stages, reproducibility of agglomeration and rupture phenomena is observed. Phenomena taking place throughout the cycled flocculation can be illustrated as shown in Figure 8.

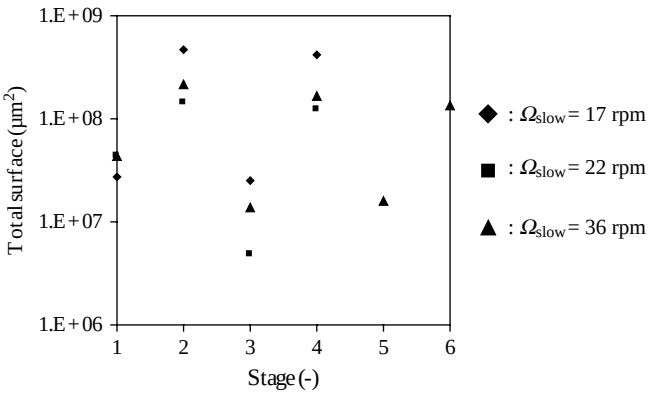

Figure 7 Variation of the total area occupied by flocs on the images during the hydrodynamic sequencing

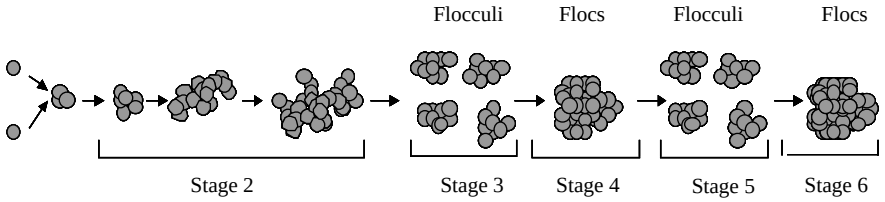

Figure 8 Schematic of the evolution of floc structure during cycled flocculation

Stage 1. The first stage of the cycled flocculation corresponds to the destabilisation of colloidal particles. Bentonite particles are destabilised and a few agglomeration phenomena occur.

Stage 2. This stage is performed under low mixing intensity. Flocs grow at a rate that is mainly determined by the mixing, the collision probability and efficiency. Nevertheless, further growth is limited by break-up induced by the hydrodynamic force exerted on the floc. This balance between growth and rupture leads to a steady-state floc size and structure. Flocs become generally large and quite loose.

Stage 3. The high mixing intensity and more precisely the eddies dissipating the energy calibrate floc size and structure. Flocculi are produced; their size is about the most probable Kolmogorov length-scale (η_{peak}).

Stage 4. *S*imilar hydrodynamic conditions to those of stage 2 are applied. At this time, agglomeration involves the flocculi formed during stage 3. The aggregates produced are smaller but denser than those derived from the flocculation stage. The resultant floc size is calibrated by the hydrodynamics and especially η_{peak}.

Stage 5. The mixing conditions of stage 3 are repeated here. Flocs stemming from the reflocculation stage are not strong enough to withstand the hydrodynamic force. Rupture phenomena occur and damage the links between the flocculi. Thus, when a floc breaks up, the daughter particles are the flocculi and not newly formed aggregates. As a consequence, the whole population of flocculi is regenerated. This explains why the floc size distributions of stages 3 and 5 are so similar.

Stage 6. The population at the beginning of stage 6 is analogous with that of stage 4. Thus, agglomeration leads to the same most probable floc size at steady-state. Therefore, this work adds weight to other investigations which provide high evidence for a multilevel floc structure (Clark and Flora, 1991).

Hydrodynamic conditioning

In the case of aluminium–bentonite flocs and fixed physico-chemical conditions, the present work shows that a break-up step changes the floc size and structure by inducing the formation of flocculi.

Flocculi and floc size after regrowth follows the Kolmogorov length-scale.

This micro-scale is linked to the dissipation of the turbulent kinetic energy and to the power dissipated (P) in the reactor. Indeed,

$$\eta = (\nu^3/\varepsilon)^{1/4} \quad \text{and} \quad \varepsilon = P/\rho V$$

where V is the volume of liquid in the reactor and ρ is the density of the fluid. Consequently, by programming a high hydrodynamic stress after a flocculation period, it

is possible to achieve an hydrodynamic conditioning of aluminium–bentonite flocs. In particular, the structure becomes denser and sizes of both flocculi and aggregates can be controlled by an hydrodynamic parameter.

Conclusions

The evolution of floc size and structure was monitored by image analysis during a cycled flocculation in a Taylor–Couette reactor. Results suggest that the flocculation process is very sensitive to initial population conditions. Flocs formed during flocculation periods are larger and looser than flocs formed during a reflocculation stage. After a break-up stage, flocs are denser, their size is controlled by hydrodynamics and reversibility of agglomeration and rupture phenomena is highlighted. Finally, it appears that cycled flocculation may be an efficient method for production of dense flocs and size-calibrated aggregates.

References

Bouyer, D., Liné, A. and Do-Quang, Z. (2004). Experimental analysis of floc size distribution under different hydrodynamics in a mixing tank. *AIChE J.*, **50**(9), 2064–2081.

Coufort, C. (2004). *Analyse expérimentale de la floculation en réacteur de Taylor–Couette: influence de l'hydrodynamique sur les phénomènes d'agglomération et de rupture,* PhD thesis. Institut National des Sciences Appliquées de Toulouse, France.

Clark, M.M. and Flora, J.R.V. (1991). Floc restructuring in varied turbulent mixing. *J. Colloid Interface Sci.*, **147**, 407–421.

Coles, D. (1965). Transitions in circular Couette flows. *J. Fluid Mech.*, **21**, 385–425.

Francois, R.J. and Van Haute, A.A. (1985). Strength of aluminium hydroxide flocs. *Wat. Res.*, **19**, 1249–1255.

Jung, S.J., Amal, R. and Raper, J.A. (1996). Monitoring effects of shearing on floc structure using small-angle light scattering. *Powder Technol.*, **88**, 51–54.

Kataoka, K. (1986). Taylor vortices and instabilities in circular Couette flows. In *Encyclopedia of Fluid Mechanics*, Cheremisinoff, N.P. (ed.), Gulf Publishing Company, Houston, TX, USA, pp. 237–273.

Parker, D.S., Warren, A.M., Kaufman, M. and Jenkins, D. (1972). Floc break-up in turbulent flocculation processes. *ASCE J. Sanitary Div.*, **1**, 79–99.

Spicer, P.T., Pratsinis, S.E., Raper, J., Amal, R., Bushell, G. and Meesters, G. (1998). Effect of shear schedule on particle size, density and structure during flocculation in stirred tanks. *Powder Technol.*, **97**, 26–34.

Tambo, N. and Watanabe, Y. (1979). Physical characteristics of flocs-I. The floc density function and aluminium floc. *Wat. Res.*, **13**, 409–419.

Thomas, D.G. (1964). Turbulent disruption of flocs in small particle size suspension. *AIChE J.*, **10**(4), 517–523.